

Difference in reduction properties between longitudinal dimension and elastic modulus of wood induced with aqueous NaOH treatment: modeling and analysis

Takashi Tanimoto¹ · Takato Nakano²

Received: 25 March 2015 / Accepted: 17 September 2015 / Published online: 12 October 2015
© The Japan Wood Research Society 2015

Abstract The dependence of the elastic modulus and the longitudinal contraction on the NaOH fractional concentration [NaOH], which differs from each other, was discussed based on a quantitative model analysis using the rule of mixtures, a cell wall model, and a dual-phase model consisting of crystal and amorphous phases. The elastic modulus was formulated as a function of the degree of crystallinity of the decrystallized microfibrils. The [NaOH] dependence of the calculated elastic modulus shows good agreement with the experimental results in that the [NaOH] dependence differs before and after at [NaOH] = 0.12. The model analysis illustrates that the reduction property of the elastic modulus is dependent on whether the amorphous region created with the treatment transverses the originally crystalline region of the microfibrils or not: the concentration is [NaOH] = 0.12. This is attributed to the difference in the reduction property between the elastic modulus and the dimensional changes along the longitudinal axis of a wood sample at [NaOH] < 0.12.

Keywords Mercerization · Elastic modulus · Contraction · Modeling · Simulation

Introduction

NaOH treatment is well-known as mercerization that is the pretreatment of cellulose, by which the cellulose crystalline structure translates from cellulose I to cellulose II in the specified concentration region. Decrystallization and swelling perpendicular to the longitudinal axis of the cellulose chains are important factors in the mercerization process, and have thus been noted and discussed for NaOH treatment. However, structural changes along the longitudinal axis of the microfibrils of a decrystallized region have been little noted with a few reports [1–4]. Nakano et al. [5–7] have reported that dimensions of wood sample induced with NaOH treatment change anisotropically, which is related to the longitudinal structural changes in the microfibrils embedded in the matrix of the wood cell wall. Ramie fibers also show significant contraction along the length of the material [8]. Changes in such shapes are due to the construction of the microfibrils, that is, the entropy elasticity force resulting from the temperature dependence [5, 8, 9].

In the present work, the authors focus on the interesting fact found in the stress relaxation properties of wood samples treated with NaOH solution [10]. That is, the [NaOH] dependence of the elastic modulus in bending differs from that of a dimensional change: the former causes changes over the [NaOH] region which consists of two regions, whereas the latter remains unchanged at [NaOH] < 0.12. This difference of [NaOH] dependences between the both is not elucidated and the mechanism of [NaOH] dependence of elastic modulus is also not clarified. Considering the decrystallization of cellulose microfibrils through NaOH treatment [7, 8, 11], the change in elastic modulus is also related to that of the crystallinity of microfibrils in the wood. As the conversion from cellulose I

✉ Takato Nakano
tnakano@kais.kyoto-u.ac.jp

¹ Asahi Woodtech Company, Chuoh-ku, Osaka 541-0054, Japan

² Professor Emeritus, Kyoto University, Kita-Shirakawa, Kyoto 606-8502, Japan

to cellulose II through NaOH treatment hardly occurs in cell walls of a wood block, the difference does not relate to the conversion. In this connection, we report the interesting fact that the mechanically isolated single tracheid do convert from cellulose I to cellulose II through the NaOH treatment, although they have the same matrix content as the wood block [9].

The elucidation in the present work will provide useful information regarding the decrystallization process of microfibrils in wood when applying NaOH treatment.

Materials and methods

Sample and measurement of elastic modulus

Samples with dimensions of 7.5 (R) × 2 (T) × 70 (L) mm were prepared from Yezo spruce (*Picea jezoensis*); here, R, T, and L indicate the radial, tangential, and longitudinal axes, respectively. The samples were then soaked in an aqueous NaOH solution with 0–0.20 fraction contents (0–20 %) after drying under a vacuum at 60 °C overnight. They were then washed in distilled water for more than 2 weeks after being stored at room temperature for 2 days. Their changes in R, T, and L dimensions were measured and subjected to a bending measurement.

The bending measurement was carried out in a chamber at room temperature under wet conditions. The wet condition was adopted to avoid the effects of change in sample shape after drying on calculation of the elastic modulus, because shape of samples treated with NaOH solution, especially samples treated at [NaOH] ≥ 0.12, significantly deforms after drying. This condition also allows the effect of lateral swelling of the microfibrils induced with NaOH treatment on the sample deformation to be negligible.

A load was supplied to the LR-plane. The elastic modulus in bending of the samples was calculated from a linear region in a stress–strain curve, which was conducted during three-point center-concentrated load bending with a 50-mm span.

Crystallinity of wood microfibrils

X-ray diffraction data were obtained on the LR-plane at 40 kV, 40 mA, and 2°/min to determine the degree of crystallinity of the wood samples, C_w , which was calculated from the diffraction profile as a fraction of the crystalline reflection area to the gross area within a scanning range of 5–35°. In our modeling, the elastic modulus is described as a function of the crystallinity in the originally crystalline region in the microfibrils, ξ , where it is decrystallized through aqueous NaOH treatment.

Results and discussion

The [NaOH] dependence of the elastic modulus and dimensional change in the NaOH treatment

Stress–strain curves of samples treated with NaOH solutions at various [NaOH] were similar to the results in the previous report [12], where stress–strain in tension was measured for sliced veneers of the same wood species. Figure 1a, b shows the elastic moduli and the dimensional changes along the length of treated wood samples as functions of NaOH concentration [NaOH] and the relative crystallinity of microfibrils, respectively. Interestingly, the modulus of the treated samples significantly decreases at [NaOH] > 0.12 after a slight reduction at [NaOH] ≤ 0.12, and then gradually decreases again at [NaOH] > 0.15, whereas the dimension along the length does not change up to [NaOH] = 0.11, and then decreases significantly. The crystallinity dependence also differs from each other. The difference between the elastic modulus and the

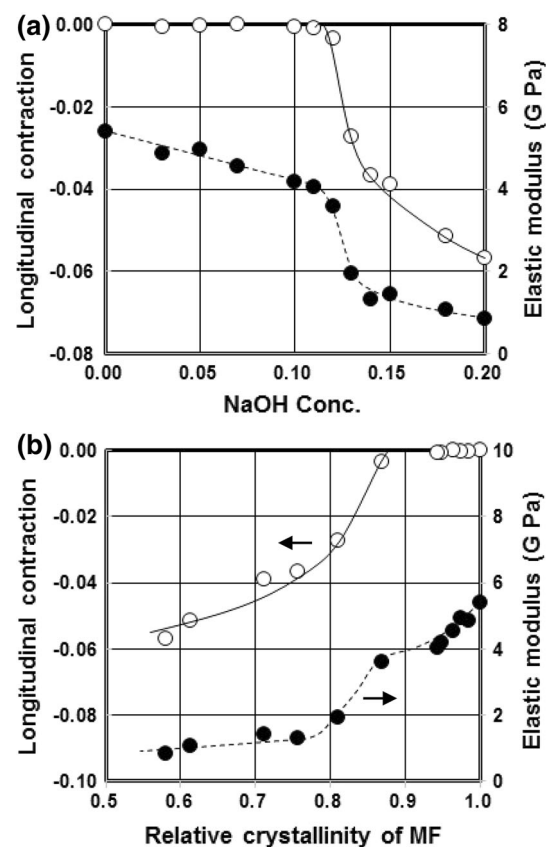


Fig. 1 Dependence of dimensional changes and elastic modulus in the longitudinal direction of wet samples on the NaOH concentration (a) and the relative crystallinity of microfibrils, MF, (b)

dimensional change is clear for $[\text{NaOH}] < 0.12$ and the degree of crystallinity > 0.87 .

Nakano et al. [5] and Nakano [7] pointed out that the dimensional changes with NaOH treatment are primarily due to the decreasing crystallinity along the longitudinal axis of the microfibrils, thereby inducing dimensional changes along the longitudinal axis of the wood sample because of the entropy elastic force. Considering this mechanism, we should note in Fig. 1 that a dimensional change starts at $[\text{NaOH}] > 0.12$, whereas the elastic modulus reduces over the $[\text{NaOH}]$ range and its reduction is divided into two regions at $[\text{NaOH}] = 0.12$. Considering eluviation of matrix components such as hemicellulose was almost completed at $[\text{NaOH}] < 0.03$ in the present treatment, we should expect the decrystallization and the change in microfibril angle (MA) as factors related to the difference between the change in the elastic modulus and dimensional change, particularly at $[\text{NaOH}] < 0.12$. However, the latter is negligible for our discussion, because the change in MA induced with the NaOH treatment was from 13 to 17° for Yezo spruce [13] so that such a slight change in this MA region had little influence on the longitudinal modulus [14]. This implies that the decrystallization induced with the NaOH treatment has different effect on the change in the elastic modulus and dimensional change, particularly at $[\text{NaOH}] < 0.12$.

We believe that the different effects are related to the decrystallization process and are based on the location of the decrystallization generated with the NaOH treatment. We therefore tried to examine the process of decrystallization with NaOH treatment using the rule of mixtures [e.g., 15, 16], a cell wall model, and a dual-phase model consisting of crystal and amorphous phases [e.g., 2, 17–19].

Relationship between elastic modulus of wood and microfibrils

First, to analyze the $[\text{NaOH}]$ dependence of the modulus of the entire wood sample related to the amorphous region generated with the NaOH treatment, the elastic modulus of the entire sample needs to be represented as a function of the volume fraction of the microfibrils. This is formulated using the knowledge regarding the microstructure and the cell wall structure of the wood.

A derivation of the elastic modulus of an entire wood sample has been attempted based on both the wood itself and its cell structure using various procedures. The elastic modulus of an entire wood sample can be derived using the rule of mixtures when assuming that the wood consists of two phases: pores and wood substance [18].

$$E = (\rho/\rho_s)^\alpha E_s, \quad (1)$$

where E and E_s are the elastic moduli of the entire wood sample and wood substance itself, respectively; ρ and ρ_s are the density of both, and α is a structural parameter. The front factor in Eq. (1), ρ/ρ_s , is equal to the volume fraction of the wood substance. Structural parameter α reflects the cell structure of the wood, such as the cell arrangement. For example, $\alpha = 1$ for loading along the longitudinal stress axis, $\alpha = \text{ca. } 1.1$ for the radial, $\alpha = \text{ca. } 1.4$ for the tangential [18]. In the present work, $\alpha = 1$ owing to the stress or strain along the longitudinal axis.

Next, we derive the elastic modulus of wood cell substance, E_s . The cell wall of the wood consists of primary and secondary walls which have three layers, S1, S2, and S3, as shown in Fig. 2, which shows a schematic of the wood cell structure (Fig. 2a) and an S2 layer regarding a cell wall as a board (Fig. 2b). We can approximately deal with the longitudinal elastic modulus in the two-dimensional space. The volume fraction of the S2 layer in the cell wall is 80 %, and thus the mechanical properties of the wood, particularly softwood, are mostly governed by the S2 layer. Additionally, the MA of S2 layer is so small, whereas those of S1 and S3 layers are at nearly a right angle. The longitudinal elastic modulus of softwood is thus governed by the S2 layer. We therefore assume that the longitudinal elastic modulus of the wood substance is approximately equal to that of the S2 layer: $E_s \approx E_L^{S2}$. This assumption also holds for treated samples as mentioned above, that is, the MA and its change induced with NaOH treatment is negligible in our discussion.

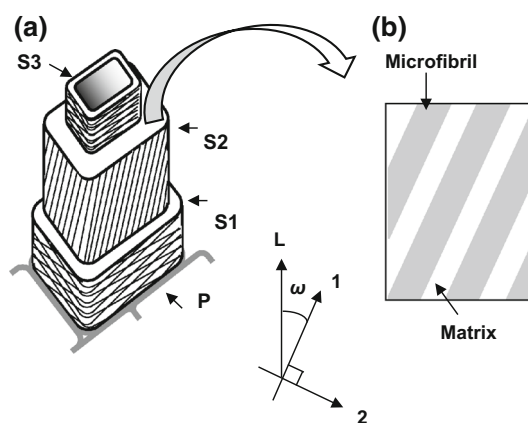


Fig. 2 A schematic of the wood cell structure (a) and the microfibrils and matrix in an S2 cell wall (b). P , $S1$, $S2$, and $S3$ indicate the primary wall and secondary walls 1, 2, and 3, respectively; in addition L , 1, 2, and ω indicate the longitudinal direction of the wood, the longitudinal direction of the microfibrils, the cross-section direction of the microfibrils, and the microfibril angle

The elastic modulus of the S2 layer along the longitudinal axis of an entire wood sample, E_L^{S2} , is represented using the anisotropic elastic theory [19],

$$E_L^{S2} = [(1/E_1) \cos^4 \omega + (1/G - 2\mu_{12}/E_1) \sin^2 \omega \cdot \cos^2 \omega + (1/E_2) \sin^4 \omega]^{-1}, \tag{2}$$

where ω is the microfibril angle, E_1 and E_2 are the elastic moduli of the S2 layer along the longitudinal and perpendicular axes of the microfibril, respectively; G is the shear rigidity, and μ_{12} is the Poisson's ratio (Fig. 2b). Here, the microfibril angle ω in our work are so slight that approximately,

$$E_L^{S2} \approx [1/E_1 + \omega^2/G]^{-1} \approx E_1. \tag{3}$$

Considering Eqs. (1), (3) and assumption $E_s \approx E_L^{S2}$, the following equation is obtained for the elastic modulus along the longitudinal, E_L :

$$E_L = \zeta(\rho/\rho_s)E_1, \tag{4}$$

where ζ is the volume fraction of the S2 layer in the cell wall and $\zeta \approx 0.8$, as mentioned above.

As shown in Eq. (4), the elastic modulus of an entire wood sample along the longitudinal axis, E_L , is reduced to the elastic modulus of the S2 layer along the longitudinal axis of microfibrils, E_1 . In the S2 layer, the microfibrils and matrix are parallel to each other in the longitudinal direction. Additionally, the microfibrils consist of crystalline and amorphous regions of cellulose chains. Thus, we consider a schematic combination mode, as shown in Fig. 3, where the amorphous region created with the NaOH treatment is added. We should note that these regions, i.e., the matrix, cellulose crystal, and amorphous regions, are not clearly distinguished, and that Fig. 3 does not show a

real structure but rather the resultant combination mode in the S2 layer. Thus, E_1 is represented by

$$E_1 = (1 - \theta) \cdot E_a + \theta \cdot \{(1 - \phi) \cdot E_{ca} + \phi \cdot E_{cc}\}, \tag{5}$$

where E_a , E_{ca} , and E_{cc} are the elastic moduli of the matrix and the originally amorphous and crystal regions of the microfibrils, respectively, and θ and ϕ are the volume fraction of the microfibrils and its crystalline region. As a result, the following equation is obtained.

$$E_L = \zeta(\rho/\rho_s)[(1 - \theta) \cdot E_a + \theta \cdot \{(1 - \phi) \cdot E_{ca} + \phi \cdot E_{cc}\}]. \tag{6}$$

Substituting values under dry condition, $E_a = 6$ GPa [20], $E_{ca} = 20$ GPa [21], $E_{cc} = 134$ GPa [22], $\theta = 0.5$, $\phi = 0.7$, $\rho_s = 1.50$, $\zeta = 0.8$, and $\rho = 0.37$ (the density of Yezo spruce) in Eq. (6) yields about 10 GPa. This value is near to the elastic modulus of Yezo spruce along the longitudinal axis. This calculation adopts the crystallinity of the microfibrils, i.e., $\phi = 0.7$, which was reported for various plants by Abe et al. [23]. The value that is generally used, i.e., $\phi = 0.55$, results in ca. 9 GPa, which is also near to the experimental value of Yezo spruce. This shows validity of Eq. (6).

Our interest is the value of elastic modulus after decrystallization. When the decrystallization proceeds, the elastic modulus of the originally crystal region with the amorphous region created with the NaOH treatment, E_{ccc} , replaces E_{cc} in Eq. (6). Then, derivation of E_L is reduced to that of E_{ccc} .

Derivation of the elastic modulus of decrystallized microfibrils based on the two-phase model

As mentioned previously, the decrystallization feature with NaOH treatment may have an influence on the elastic modulus of the entire wood sample, i.e., the locations of the crystal and amorphous regions in the microfibrils should govern the elastic modulus. This combination likely explains the difference between the dimensional changes and the elastic modulus along the longitudinal axis of the wood at $[\text{NaOH}] < 0.12$, as shown in Fig. 1, because the parallel residual crystalline region might influence the dimensional changes along the longitudinal axis of the microfibrils much more than the elastic modulus. From this viewpoint, we analyzed the elastic modulus of an entire wood sample along the longitudinal axis using the proposed model.

Assuming that the NaOH solution attaches to periodical defects along the longitudinal axis of the microfibrils and then diffuse into the originally crystalline region [5, 8], the decrystallization in the longitudinal section of a microfibril proceeds during the NaOH treatment as shown schematically in Fig. 4, in which is shown the two types of distribution of the amorphous region created through the treatment (Fig. 4c, d). When this decrystallization

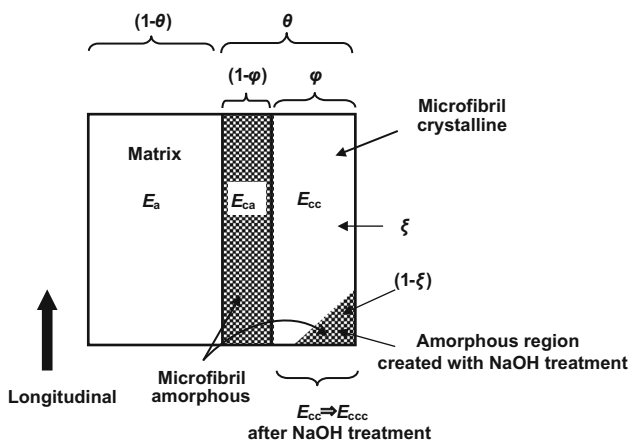


Fig. 3 A schematic of the combination mode for the matrix (symbol a) and crystalline (symbol cc) and amorphous (symbol ca) regions of a microfibril

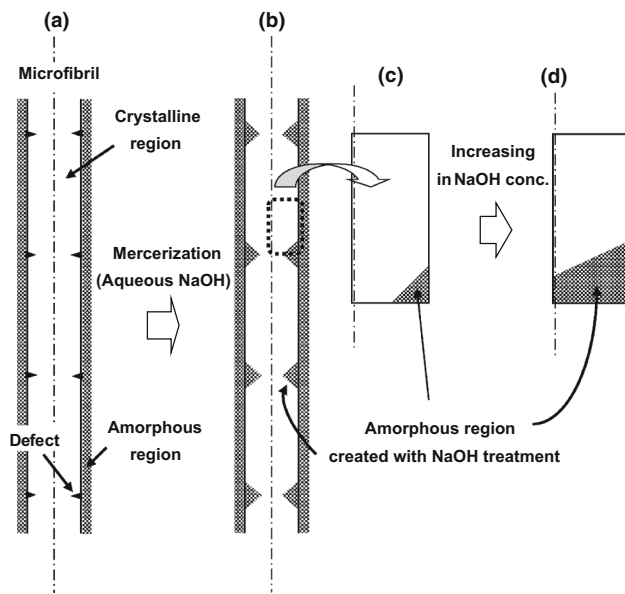


Fig. 4 A schematic of the change in longitudinal section of the microfibril during mercerization: **a** untreated microfibril; **b** after mercerization; **c** enlarged view before traversing crystal region; **d** enlarged view after traversing crystal region

proceeds, E_{cc} should be represented as a function of ξ which is the degree of crystallinity of the originally crystalline region in microfibrils: $\xi = 1$ for an untreated microfibril.

Under our experimental conditions, the stress direction is approximately parallel to both the microfibrils and matrix as mentioned above. In the following discussion, the matrix, amorphous and crystalline regions of a microfibril are indicated by subscripts a, ca and cc, respectively. The amorphous region after the NaOH treatment consists of two regions, i.e., the originally amorphous region and the new amorphous region created in the original cc region through the NaOH treatment. Our interest is on the latter region. We expect that the new amorphous region has two types of distribution shown as a cylindrical model of a microfibril in Fig. 5a, b. The distribution of an amorphous region created through the NaOH treatment should depend on the diffusion of the NaOH solution.

To simplify our discussion, we regard the originally crystalline region of microfibrils as a cylinder and discuss the diffusion of aqueous NaOH using a plane through the center line. According to the cylindrical model, the distribution of a solution concentration is represented by a monotonically decreasing function of a position from the surface to the center after a sufficient period of time under a constant concentration on the boundary surface [24]. In our case, the solution does not uniformly diffuse from the boundary surface with constant concentration but from the located defect, so that the distribution cannot simply be

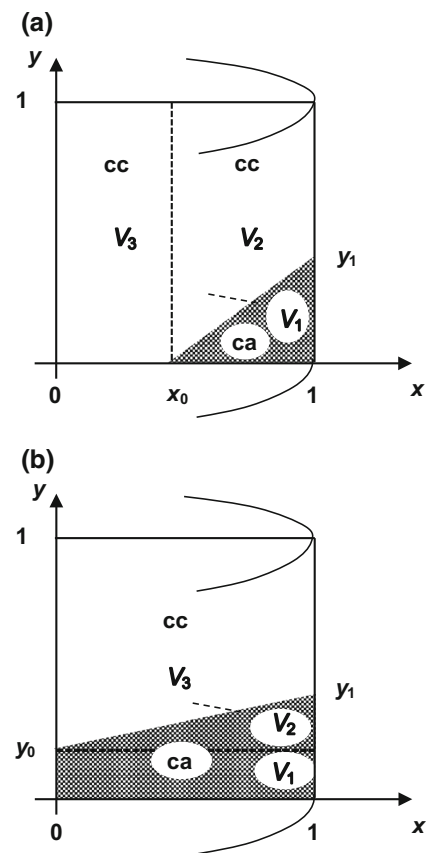


Fig. 5 The distribution modes of an amorphous region in a microfibril created through NaOH treatment. **a**, **b** are the distributions of non-traversing and traversing microfibrils, respectively

described. However, the distribution is expected to be monotonic from the surface to the center. We thus assume that the distribution of the amorphous region created with diffusion of aqueous NaOH is linearly decreasing from the surface to the center in the local region on the plane of the longitudinal section.

We consider two types of distribution for the amorphous region created in the originally crystalline region, where the mesh pattern on a plane through the x and y axes indicates an amorphous region created through the NaOH treatment (Fig. 5a, b): the applied force acts along the y axis under loading. The difference between these two types is whether the amorphous region transverses the originally crystalline region of the microfibrils or not. Figure 5a, b shows a continuous crystalline region along the longitudinal axis of the microfibrils, and the absence of such a region, respectively. The x axis is the position from the surface of the microfibrils; $x = 0$ and $x = 1$ indicate the center and surface in the originally crystalline region, respectively. The y axis is the longitudinal position of amorphousness generated with the NaOH treatment (see Fig. 4). The value on y coordinate at the center and surface is y_0 and y_1 , respectively.

In Fig. 5a, $y_0 = 0$ and $y_1 = a$ constant value, the decrystallization proceeds up to $x = x_0$. The regions shown in Fig. 5a, b are divided into three regions to calculate the volume of the amorphous and crystal regions. The volume of the three regions shown in Fig. 5a, the created amorphous, residual crystalline, and originally crystalline regions, are V_1 , V_2 , and V_3 , respectively. In Fig. 5b, the volume are the flatly amorphous region (V_1), the slantingly amorphous region (V_2), and the residual crystalline region (V_3).

First, we discuss how to determine ξ necessary to calculate E_{ccc} . According to Norimoto and Takabe [25] and Abe and Yano [23], the weight fraction of both the microfibrils in wood and crystal region in microfibril are $\theta_w = 0.5$ and $\varphi_w = 0.7$, respectively. Thus, the crystallinity of a gross wood, C_w , is represented by

$$C_w = \theta_w \cdot \phi_w \cdot \xi = 0.35\xi. \tag{7}$$

Thus,

$$\xi = 2.86C_w. \tag{8}$$

As the measurement value, C_w , is not necessarily true, we introduce the correction term, m ;

$$\xi = 2.86mC_w. \tag{9}$$

Thus, using the measurement value, C_w , we can determine parameter m by a best-fitting simulation, so that we obtain the crystallinity of the originally crystal region cc created with the NaOH treatment, ξ , as a function of C_w .

Next, we discuss the distribution type shown in Fig. 5a. Applying the rule of mixtures to this combination, the elastic modulus along the longitudinal direction (y axis), E_{ccc} , is represented by

$$E_{ccc} = (V_3/V)E_{cc} + (1 - V_3/V) \left[\left\{ \frac{(V_1/V)}{(1 - V_3/V)} \right\} \times (1/E_{ca}) + \left\{ 1 - \frac{(V_1/V)}{(1 - V_3/V)} \right\} (1/E_{cc}) \right]^{-1}, \tag{10}$$

$$\times (V = V_1 + V_2 + V_3)$$

where $V_1/V = (y_1/3)(2 - x_0 - x_0^2)$ and $V_3/V = x_0^2$ from calculation of the each volume shown in Fig. 5a. As the density of the amorphous and crystal regions in microfibrils are nearly equal, which are 1.47 and 1.59, respectively [14], we can regard the volume fraction as the weight fraction. Thus, the crystallinity in the region cc, ξ , is approximately represented by

$$\xi = 1 - V_1/V = 1 - (y_1/3)(2 - x_0 - x_0^2). \tag{11}$$

Thus, Eq. (10) reduces to

$$E_{ccc} = x_0^2 E_{cc} + (1 - x_0^2) \left[\left\{ \frac{(1 - \xi)}{(1 - x_0^2)} \right\} (1/E_{ca}) + \left\{ 1 - \frac{(1 - \xi)}{(1 - x_0^2)} \right\} (1/E_{cc}) \right]^{-1}. \tag{12}$$

As we approximate that the distribution of the amorphous region decreases monotonically from the surface to the center, we put

$$y_1 = k(1 - x_0). \quad (k = \text{constant}). \tag{13}$$

Substituting Eq. (13) into Eq. (11), we have the following equation after approximately solving a quadratic equation:

$$x_0 \cong 2/3 - (1 - \xi)/k. \quad (x_0 < 1). \tag{14}$$

Thus, E_{ccc} described by Eq. (12) is confirmed which has parameters m and k . Accordingly, we obtain E_L by putting E_{ccc} instead of E_{cc} in Eq. (6): E_L has also parameters m and k .

Another distribution shown in Fig. 5b is easily obtained. Considering that the amorphous ($V_1 + V_2$) and crystal (V_3) regions are combined in series, we have the following equation immediately,

$$E_{ccc} = [(1 - \xi)/E_{ca} + \xi/E_{cc}]^{-1}. \tag{15}$$

Thus, we obtain E_L by the same procedure as from Eq. (12), which has only one parameter m .

The parameters m and k are determined by a best-fitting simulation using experimental data and E_L calculated from Eqs. (12) and (15) derived above.

Simulation results and validity of modeling

Equations (12) and (15) were derived by assuming that the cause of the reduction with increasing [NaOH] (or with decreasing in the crystallinity) is due to the combination of the crystal and amorphous regions through NaOH treatment. Applying Eqs. (12) and (15) to below and above [NaOH] = 0.12, respectively, the calculation results were fitted to the experimental results. Considering experimental data under wet condition [20], the values in Eq. (6) are $E_a = 2$ GPa, $E_{ca} = 5$ GPa under, $E_{cc} = 134$ GPa, $\theta = 0.5$, $\varphi = 0.7$, $\xi = 0.8$, $\rho_s = 1.50$, and $\rho = 0.37$.

The solid lines in Fig. 6 show the best fitting of the simulation as functions of the [NaOH] (Fig. 6a) and the relative crystallinity of the microfibrils based on the value at [NaOH] = 0.00 (Fig. 6b), respectively. The simulation results are not perfect, but are mostly in agreement with the experimental results. The best-fitting value of parameter were $m = 0.849$ and $k = 0.610$. We find that a reduction of the elastic modulus occurs over [NaOH], which is divided into two parts at [NaOH] = 0.12: the reduction at a lower [NaOH] is graduate and the other remarkable.

Cause of the difference between the elastic modulus and dimensional changes

The agreement between the calculation and experimental results shown in Fig. 6 implies that the amorphous region

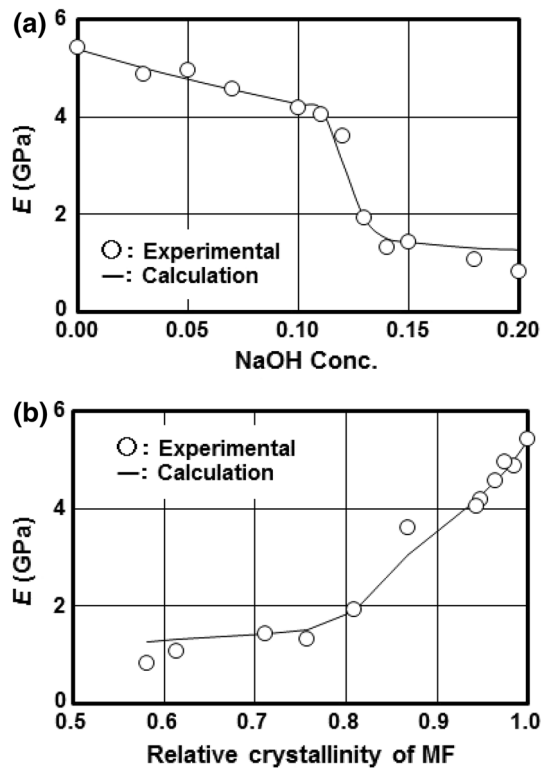


Fig. 6 Comparison of the experimental and calculation results regarding the elastic modulus of wet samples: **a** versus NaOH concentration and **b** versus the relative crystallinity in microfibrils in a wood cell wall

created through the NaOH treatment has a monotonically decreasing distribution from the surface to the center in the cc region, and that the amorphous region perfectly transverse the region at $[\text{NaOH}] > 0.12$ after increasing in $[\text{NaOH}]$ (Fig. 5a, b). This mechanism explains not only the $[\text{NaOH}]$ dependence of the elastic modulus, but also the difference in the $[\text{NaOH}]$ dependence between the elastic modulus and the dimensional changes.

A continuous crystal region along the longitudinal axis of the microfibrils remains in the cc region at $[\text{NaOH}] < 0.12$ (Fig. 5a), although the amorphous region increases with an increase in $[\text{NaOH}]$. This longitudinally continuous crystal region is sufficiently rigid to restrict the contraction by the amorphous region created with the NaOH treatment, thereby preventing the microfibrils from shrinking the wood sample, whereas such an inhibitory factor is lost at $[\text{NaOH}] > 0.12$ in which the microfibrils do easily shrink the wood sample (Fig. 5b). On the other hand, the elastic modulus gradually decreases with an increase in the degree of amorphousness, as represented in the above equations. However, the tendency of this reduction changes at $[\text{NaOH}] > 0.12$ because of the significantly different contribution of the decrystallization between below and above $[\text{NaOH}] = 0.12$.

Conclusion

A reduction of the elastic modulus occurs through NaOH treatment, and is divided into two parts at $[\text{NaOH}] = 0.12$. This reduction mechanism was described based on a quantitative analysis using the rule of mixtures, a cell wall model, and a dual-phase model consisting of crystal and amorphous phases, and the difference between the $[\text{NaOH}]$ dependence of the dimensional and elastic modulus changes was then discussed.

Two equations describing the elastic modulus of a wood sample were derived by assuming that the cause of this reduction is due to the combination of the crystal and amorphous regions in microfibrils created with NaOH treatment. Applying these equations to below and above $[\text{NaOH}] = 0.12$, they were not perfect but were mostly in agreement with the experimental results.

References

1. Jeffries R, Warwicker JO (1969) The function of swelling in the finishing of cotton. *Text Res J* 1:548–559
2. Schniewind AP (1972) Elastic behaviour of the wood fiber. In: Jayne BA (ed) *Theory and design of wood and fiber composites materials*. Syracuse University Press, New York, pp 83–96
3. Stöckmann VE (1971) Effect of pulping on cellulose structure Part I. *Tappi* 54:2033–2037
4. Stöckmann VE (1971) Effect of pulping on cellulose structure Part II. *Tappi* 54:2038–2045
5. Nakano T, Sugiyama J, Norimoto M (2000) Contraction force and transformation of microfibril with aqueous sodium hydroxide solution. *Holzforchung* 54:315–320
6. Ishikura Y, Nakano T (2007) Contraction of the microfibrils of wood treated with aqueous NaOH. *J Wood Sci* 53:175–177
7. Nakano T (2010) Mechanism of microfibril contraction and anisotropic dimensional changes for cells in wood treated with aqueous NaOH solution. *Cellulose* 17:711–719
8. Nakano T, Tanimoto T, Hashimoto T (2013) Morphological change induced with NaOH-water solution for ramie fiber: change mechanism and effects of concentration and temperature. *J Mater Sci* 48:7510–7517
9. Nakano S, Nakano T (2015) Morphological changes induced in wood samples by aqueous NaOH treatment and their effects on the conversion of cellulose I to cellulose II. *Holzforchung* 69:483–491
10. Tanimoto T, Nakano T (2013) Side-chain motion of components for wood samples partially non-crystallized with NaOH aqueous solution. *Mater Sci Eng C* 33:1236–1241
11. Fengel D, Jakob H, Strobel C (1995) Influence of the alkali concentration on the formation of cellulose II. *Holzforchung* 49:505–511
12. Nakano T (1989) Plasticization of wood by alkali treatment. Relationship between plasticization and the ultra-structure. *Mokuzai Gakkaishi* 35:431–437
13. Fujimoto T, Nakano T (2000) The effect of mercerization on wood structure features (in Japanese). *Mokuzai Gakkaishi* 46:238–241
14. Watanabe U, Norimoto M (2000) Three dimensional analysis of elastic constants of the wood cell wall. *Wood Res* 87:1–7

15. Hill R (1964) Theory of mechanical properties of fiber-strengthened materials. 1. Elastic behavior. *J Mech Phys Solids* 12:199–212
16. Habip LM (1965) A review of recent work on multilayered structures. *Int J Mech Sci* 7:589–593
17. Tang RC, Hsu NN (1973) Analysis of the relationship between microstructure and elastic properties of the cell wall. *Wood Fiber* 5:139–151
18. Ohgama T, Yamada T (1974) Elastic modulus of porous materials (in Japanese). *Mokuzai Gakkaishi* 20:166–171
19. Lekhnitskii SG (1963) Theory of elasticity of an anisotropic elastic body. Holden-Day, San Francisco, pp 1–73
20. Cousins WJ (1978) Young's modulus of hemicellulose as related to moisture content. *Wood Sci Technol* 2:161–167
21. Gindl W, Martinschitz KJ, Boesecke P, Keckes J (2006) Changes in the molecular orientation and tensile properties of uniaxially drawn cellulose films. *Biomacromolecules* 7:3146–3150
22. Sakurada I, Nukushina Y (1962) Experimental determinations of the elastic modulus of crystalline regions in oriented polymers. *J Polym Sci* 57:651–660
23. Abe K, Yano H (2009) Comparison of the characteristics of cellulose microfibril aggregates of wood, rice straw and potato tuber. *Cellulose* 16:1017–1023
24. Crank J (1975) The mathematics of diffusion, 2nd edn. Oxford Sci Publication, New York, pp 44–68
25. Norimoto M, Takabe K (1985) On noncrystalline structure of wood. *Wood Res Tech Notes* 21:96–101